ACS APPLIED MATERIALS & INTERFACES

Research Article

www.acsami.org

Enhanced Antibacterial Activity of Silver/Polyrhodanine-Composite-Decorated Silica Nanoparticles

Jooyoung Song, Hyunyoung Kim, Yoonsun Jang, and Jyongsik Jang*

WCU Program of Chemical Convergence for Energy and Environment (C2E2), School of Chemical and Biological Engineering, College of Engineering, Seoul National University, 599 Gwanak-ro, Gwanak-gu, Seoul 151-742, Korea

Supporting Information

ABSTRACT: This work describes the synthesis of silver/polyrhodanine-composite-decorated silica nanoparticles and their antibacterial activity. Polymerization of polyrhodanine proceeded preferentially on the surface of the silica nanoparticles where Ag^+ ions were located. In addition, the embedded Ag^+ ions were reduced to form metallic Ag nanoparticles; consequently, silver/polyrhodanine-composite nanoparticles (approximately 7 nm in diameter) were formed on the surface of the silica nanoparticles. The resulting nanostructure was investigated using electron microscopy, Fourier-transform infrared spectroscopy, ultraviolet−visible spectroscopy, and X-ray photoelectron spectroscopy. The silver/polyrhodanine-nanocomposite-decorated silica nanoparticles exhibited excellent antimicrobial activity toward gram-negative *Escherichia coli* and gram-positive *Staphylococcus aureus* because of the antibacterial effects of the silver nanoparticles and the polyrhodanine. The silver/polyrhodanine-composite nanoparticles may therefore have potential for use as a long-term antibacterial agent.

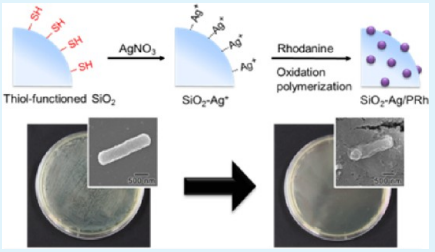

KEYWORDS: *silver nanoparticle, polyrhodanine, nanocomposite, oxidation polymerization, bactericidal agent*

INTRODUCTION

With increasing concern over microbial infections, in particular hospital-acquired infections, there is growing demand for effective and safe antimicrobial agents.[1−4] Silver and silver salts are well-known to be excellent hygienic and curative agents because of their broad-spectrum antimicrobial activity and limited microbial resistance.[5−7] A number of studies have described the antibacterial mechanism of silver nanoparticles. Silver nanoparticles showed cytotoxic effects toward microbes by generating oxidative stress[8,9] and DNA damage[10−12] as well as through interactions with cell walls.[5,13] Interestingly, Xiu et al. demonstrated that silver nanoparticles kill *Escherichia coli* by releasing silver ions from the oxidized surface.[14]

Over the past few decades, numerous silver-containing antimicrobial nanomaterials have been reported. Lv et al. reported a preparation of Ag-decorated silicon nanowires with long-term usable antibacterial activity.[15] Li et al. fabricated antibacterial thin films consisting of quaternary ammonium silane and silver nanoparticles using an aqueous layer-by-layer deposition method.[16] Recently, Lin et al. fabricated biocompatible antibacterial Ag-immobilized nanosilicate platelets using fully exfoliated clay as a carrier for the Ag nanoparticles.[17] Other materials, including graphene oxide,[18−21] carbon nanotubes,[20,21] polymer nanofibers,[22−24] polymer thin films,[16,25] and silica nanoparticles,[26,27] have been used as substrates for deposited layers containing silver nanoparticles. These nanocomposites showed enhanced antibacterial performance compared with that of colloidal silver nanoparticles because the substrates inhibited aggregation and slowed the depletion of the silver nanoparticles. Some of these substrates increased the antibacterial activity because of their own bactericidal properties.

Polyrhodanine may also have antibacterial properties owing to its tertiary amide groups. Under aqueous conditions, these tertiary amide groups can be partially protonated, developing a positive charge. Positively charged polyrhodanine has been shown in interact with the negatively charged bacterial cell wall, leading to the death of the bacteria.[28]

It has been reported that silver cations can initiate oxidation polymerization of pyrrole and aniline because of the oxidation potential for the polymerization (E = 0.8 V).[29,30] During the polymerization, the silver ions were simultaneously reduced; consequently, metallic silver nanoparticles containing polymer nanocomposites were formed. Through this reaction, silver/polymer nanocomposites can be obtained under mild reaction conditions without additional reducing agents or initiators. Previously, we reported that rhodanine, which has antibacterial properties, can also be polymerized using silver ions as an oxidation initiator.[23,31] The resulting silver/polyrhodanine nanofibers and nanotubes showed excellent antibacterial performance because of the synergistic effect of the silver and polyrhodanine. However, it remains a challenge to prepare smaller nanocomposites with a high specific surface area for enhanced antibacterial activity.

Here, we report the synthesis of silver/polyrhodanine nanocomposites on silica nanoparticles, resulting in a large

Received: June 14, 2013
Accepted: October 24, 2013
Published: October 24, 2013

Scheme 1. Schematic Illustration of the Synthetic Procedure for SiO_2−Ag/PRh Nanoparticles

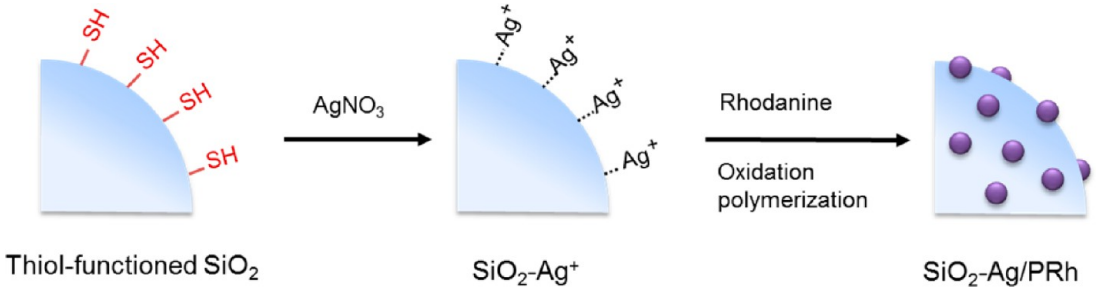

specific surface area. The polymerization of rhodanine proceeded preferentially on the silica surface, where the initiator Ag^+ ions were located. During oxidization of the rhodanine monomer, the silver ions were reduced to silver nanoparticles and formed a complex with rhodanine because of coordinative interactions,[23,28,31] resulting in a silver/polyrhodanine nanocomposite on the surface of the silica nanoparticles. We expect that this nanocomposite will exhibit antibacterial properties because of the antibacterial action of the polyrhodanine and the silver nanoparticles. To investigate the antibacterial activity of the silver/polyrhodanine-composite-decorated silica (SiO_2−Ag/PRh) nanoparticles, the viability of gram-negative *E. coli* and gram-positive *Staphylococcus aureus* was investigated in the presence of the SiO_2−Ag/PRh composite nanoparticles. The long-term stability of the nanoparticles was investigated by examining the silver-depletion properties.

EXPERIMENTAL SECTION

Materials. Silica nanoparticles of ∼50 nm in diameter were typically synthesized using tetraethyl orthosilicate and ammonia solution (28−30%). (3-Mercaptopropyl)trimethoxy silane was purchased from Aldrich (Milwaukee, WI, USA) and used as a silane-coupling agent to modify the silica surface. Rhodanine monomer, silver nitrate (99%), ethylene glycol, 1,6-hexanediamine, and ethanol were purchased from Aldrich. As silver-ion scavengers, sodium thiosulfate and sodium thioglycolate were obtained from Aldrich. To test bacterial growth, *E. coli* (ATCC 11775) and *S. aureus* (ATCC 12600) were purchased from Fisher (Tucson, AZ, USA).

Fabrication of Silver/Polyrhodanine-Composite-Decorated Silica Nanoparticles. To prepare the SiO_2−Ag/PRh nanoparticles, the prepared silica nanoparticles were pretreated with thiol-functioned silane. Silica (200 mg) was dispersed in 3 mL of ethanol solution to which 120 μL of (3-mercaptopropyl)trimethoxy silane and 150 μL of NH_4OH (30%) solution were added, and the solution was vigorously stirred at room temperature for 24 h. After centrifugation, the thiol-silane-treated silica nanoparticles were obtained and dried in a vacuum oven at 25 °C. Thiol-silica nanoparticles (50 mg) were dispersed in 30 mL of ethanol by sonication for 20 min. Silver nitrate (0.188 mmol) was introduced to the reactor and stirred for 2 h at 60 °C. Afterwards, rhodanine monomer (0.075 mmol) was introduced to the reaction medium, and the chemical oxidation polymerization of rhodanine proceeded for 24 h on the surface of silica nanoparticles at 60 °C with vigorous stirring. After polymerization, the silver/polyrhodanine-decorated silica nanoparticles were obtained by centrifugal precipitation and washed with an excess ethanol solution to remove residual reagents.

Antibacterial Test. The microorganism suspensions (*E. coli* and *S. aureus*) used for the tests contained 10^6−10^7 colony-forming units (CFU) in 1 mL. As-prepared samples (5 mg) were dispersed in 1 mL of sterilized water and inoculated with 100 μL of bacterial suspension (*E. coli* and *S. aureus*). The bacteria-inoculated solutions were incubated in a shaking incubator at 37 °C. After 1 h of contact time, 50 μL of each solution was taken and cultured on Luria−Bertani (LB) agar plates. The LB agar plates were kept at 37 °C for 24 h, and the bacterial colonies were observed.

For SEM observation, the SiO_2−Ag/PRh nanoparticles were hydraulically pressed to obtain a disc. Then, the bacterial suspension was drop-casted on the surface of the sample disc and cultivated at 37 °C for 4 h. The bacteria were then fixed in 2.5% glutaraldehyde for 2 h and rinsed carefully with distilled water. Postfixation proceeded for 1 h with 1% osmium tetroxide in distilled water. After fixation, the samples were dehydrated with ethanol (20−100%), air-dried, and sputter-coated with platinum/palladium for SEM observation.

The minimum inhibitory concentration (MIC) test was performed as follows. Sterilized LB agar solutions (5 mL) were inoculated with each bacterium (10^5−10^6 CFU). Then, the prepared nanoparticles were added to the bacteria suspensions at different concentrations and incubated at 37 °C with shaking at 150 rpm for 24 h. The growth or lack of growth was determined by visual inspection.

To test the long-term antimicrobial activity of the synthesized composite nanoparticles, an antimicrobial test was performed under silver-depletion conditions using a silver-ion scavenger. For the test, as-prepared SiO_2−Ag/PRh nanoparticles (5 mg) were dispersed in 1 mL of distilled water and neutralized with a neutralizer solution (14.6 wt % sodium thiosulfate and 10 wt % sodium thioglycolate in distilled water). The prepared neutralizer solution is known as a silver-ion scavenger.[32] To exclude the antimicrobial activity of silver nanoparticles, an adequate amount of neutralizer solution was used. After 30 min of shaking, the samples were inoculated with the 100 μL of bacterial suspension (10^6−10^7 CFU/mL). A blank aqueous solution, silver nitrate, pristine silica nanoparticles, thiol-silane-treated silica nanoparticles, and silver-nanoparticles-decorated silica SiO_2−Ag nanoparticles were also prepared as experimental controls. The bacteria-inoculated solutions were incubated in a shaking incubator at 37 °C. After 1 h, aliquots of equal volume were taken from each tube and cultured on LB agar plates. The LB agar plates were kept at 37 °C for 24 h, and the number of bacterial colonies was counted to evaluate antibacterial performance. The bacterial survival was calculated as $B/A \times 100$ (where A is the number of surviving bacteria colonies in the control and B is that in the sample). For accuracy of the results, the entire antibacterial test was conducted three times, and averaged data is presented. The standard deviation was less than 10%

Instrumentation. Transmission electron microscopy (TEM) images were obtained with a JEM-200CX (JEOL, Japan) at an acceleration voltage of 200 kV. Field-emission scanning electron microscopy (FE-SEM) images were obtained using a JEOL 6700 at an acceleration voltage of 10 kV. To prepare samples for TEM and FE-SEM characterization, the prepared nanoparticles were dispersed in water and cast onto a copper grid and silicon wafer, respectively. Fourier transform infrared (FTIR) spectra were obtained using a Bomem MB 100 spectrometer (Quebec, Canada) in absorption mode at a resolution of 4 cm^{-1} by averaging 64 scans. Ultraviolet−visible (UV−vis) spectra were acquired using a Lambda-20 spectrometer (PerkinElmer, USA). To obtain UV−Vis spectra, the samples were dissolved in *N*-methyl-2-pyrrolidone. X-ray photoelectron spectroscopy (XPS) data was obtained using Sigma Probe electron spectroscope. Thermo gravimetric analysis (TGA) was carried out in a nitrogen gas flow using a TGA 2050 analyzer (TA Instruments). The

concentrations of Ag were measured by inductively coupled plasma atomic emission spectrometry (ICP-AES).

RESULTS AND DISCUSSION

The synthesis of the SiO_2−Ag/PRh nanoparticles is illustrated in Scheme 1. First, the silica nanoparticles were pretreated with thiol-terminated silane to provide a strong affinity for metal ions.[33] Then, the thiol-functionalized SiO_2 nanoparticles were dispersed in silver nitrate dissolved in ethanol. The Ag^+ ions preferentially located on the surface of the nanoparticles because of the strong metal-binding properties of the thiol groups. Rhodanine monomer was then introduced and polymerized using the Ag^+ ions as an oxidative initiator. Because the Ag^+ ions were located on the surface of silica nanoparticles, the polymerization proceeded preferentially on the silica surface. During polymerization, the Ag^+ ions were reduced to metallic silver nanoparticles.[23,31] Following polymerization, the Ag/polyrhodanine-nanocomposite-decorated silica nanoparticles took on a dark appearance, which is attributed to the existence of polyrhodanine.

Figure 1a shows transmission electron microscope (TEM) images of the silica nanoparticles that were treated with thiol-terminated silane, and Figure 1b−d shows the synthesized SiO_2−Ag/PRh nanoparticles. As shown in the TEM images, spherical silver/polyrhodanine composites were densely loaded on the surface of silica nanoparticles, where the mean diameter of the nanoparticles was approximately 7 nm. The high-resolution (HR)-TEM data shown in Figure 1d reveals that the composite particles had a *d* spacing of 0.23 nm, which corresponds to the (111) crystal plane of silver.[34] The lattice fringe of the silver nanoparticles was blurred at the edges; this may be due to the polyrhodanine, which covers the surface of the Ag nanoparticles. These data are consistent with polyrhodanine-covered Ag nanoparticles formed on the surface of silica nanoparticles following oxidation polymerization.

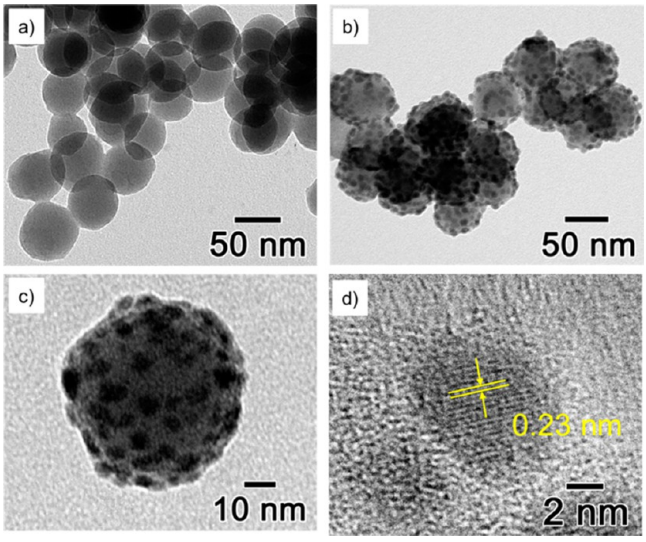

Figure 1. TEM images of (a) thiol-silane-treated silica nanoparticles and (b, c) SiO_2−Ag/PRh nanoparticles with low- and high-magnification, respectively. (d) HR-TEM image of Ag/PRh composite on the SiO_2 surface.

X-ray photoelectron spectroscopy (XPS) was carried out to investigate the silver nanoparticles on the surface of the silica nanoparticles. Metallic silver 3d peaks are typically centered at 368 eV (for Ag $3d_{5/2}$) and 374 eV (for Ag $3d_{3/2}$), with a spin-energy separation of 6.0 eV.[35,36] As shown in Figure 2a, the as-prepared SiO_2−Ag/PRh nanoparticles exhibit two sharp peaks at 368 and 374 eV. The SiO_2−Ag/PRh nanoparticles exhibited the same spin-energy separation (6.0 eV), which implies that zerovalent silver nanoparticles were formed after the reaction. Fourier-transform infrared (FTIR) and UV−vis spectra of the as-prepared samples were obtained to verify the polymerization of rhodanine. In the FTIR spectrum of SiO_2−Ag/PRh nanoparticles shown in Figure 2b, the strong peak at 1710 cm^{-1}, which is indicative of C═O stretching of the rhodanine monomer, was absent, and instead peaks were observed at 1638, 1560, and 1182 cm^{-1}. The absorbance peak at 1638 cm^{-1} was assigned to C═C stretching, the peak at 1560 cm^{-1}, to C═N^+ stretching, and the peak at 1182 cm^{-1}, to C−O^-

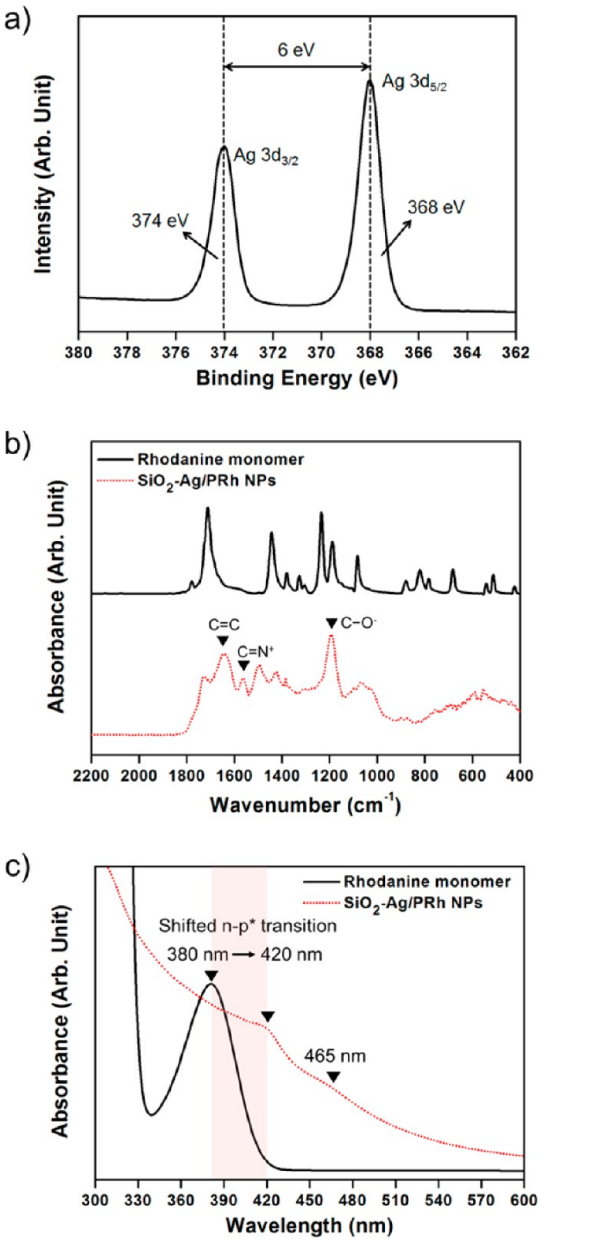

Figure 2. (a) XPS spectrum of the SiO_2−Ag/PRh nanoparticles. (b) FTIR and (c) UV−vis spectra of rhodanine monomer (black solid line) and SiO_2−Ag/PRh nanoparticles (red dotted line).

stretching of the conjugated polyrhodanine.[23,31] These FTIR spectra suggest that polymerization of the rhodanine occurred.[37] UV−vis spectra are shown in Figure 2c. Prior to polymerization, the rhodanine monomer showed an absorption peak at around 380 nm, which is attributed to an n−p* transition of the rhodanine monomer.[37] However, the polymerized sample showed absorption peaks at 420 and 465 nm, and the peak at 380 nm was absent. The absorption peak at 420 nm may be due to the red-shifted n−p* transition of rhodanine because of silver-binding complexes. More importantly, the peak observed near 465 nm is attributed to the polymeric backbone of the synthesized polyrhodanine.[31,37] On the basis of these data, we concluded that the oxidation polymerization of rhodanine using silver ions as an initiator was successful. The SiO_2−Ag/PRh nanoparticles were analyzed using thermogravimetric (TGA) and inductively coupled plasma (ICP) analyses, which showed that the nanoparticles were composed of 15% polyrhodanine and 1.4% silver by weight.

The SiO_2−Ag/PRh nanoparticles were expected to exhibit antibacterial activity because of the silver and polyrhodanine at the surface. We evaluated the antibacterial activities of the SiO_2−Ag/PRh nanoparticles toward *E. coli* and *S. aureus*. Samples (5 mg) were dispersed in 1 mL of distilled water and inoculated with bacteria at a concentration of 10^5−10^6 CFU per mL. A control aqueous solution was prepared with the bacteria but without nanoparticles. After a contact time of 1 h, each solution was sampled and cultured on LB agar plates. As shown in Figure 3, after 24 h of incubation, dense bacterial colonies were observed on the control LB agar for both *E. coli* (Figure 3a) and *S. aureus* (Figure 3c). However, the LB agar plates with the SiO_2−Ag/PRh nanoparticles exhibited no growth of bacterial colonies, indicating excellent antibacterial activity against both strains of bacteria (Figure 3b,d).

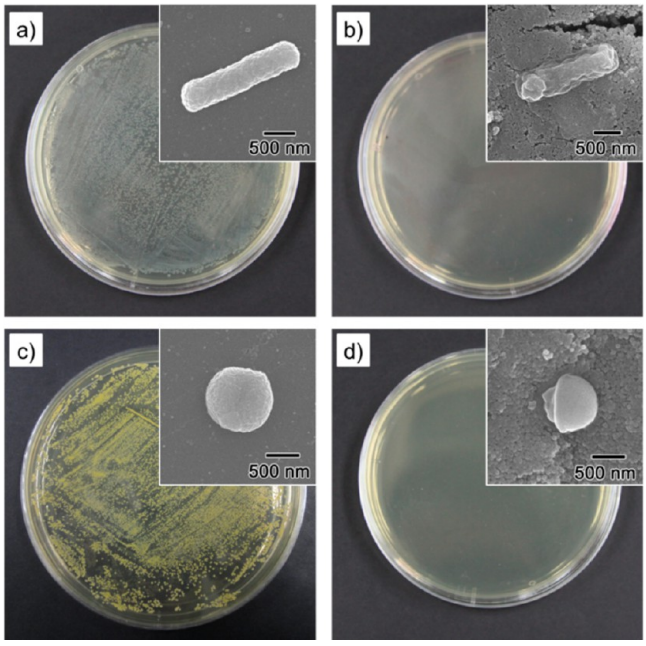

Figure 3. Photographs of colonies of (top) *E. coli* and (bottom) *S. aureus* (a, c) without nanoparticles treatment and (b, d) treated with SiO_2−Ag/PRh nanoparticles. Inset figures shows the FE-SEM images of a single bacterial cell (left) in the absence of bactericidal agents and (right) treated with the as-prepared nanoparticles.

Morphological changes in the bacteria were observed following exposure to the SiO_2−Ag/PRh nanoparticles using field-emission scanning electron microscopy (FE-SEM), as shown in the inset of Figure 3. *E. coli* exhibited damage on the outer membrane, with a loss of the intact rod-like shape. Similarly, *S. aureus* shrunk and lost its spherical shape following exposure to the nanoparticles, which is consistent with damage to the cell wall. Minimum inhibitory concentration (MIC) tests were carried out on both bacteria. The MIC of the nanoparticles against *E. coli* was 1.5 mg mL^{-1} and that toward *S. aureus* was 2.5 mg mL^{-1}. These data suggest that the SiO_2−Ag/PRh nanoparticles are effective antibacterial agents against both gram-positive and gram-negative bacteria.

The tenacity of the Ag/PRh nanoparticles on the silica surface was assessed from TEM images of the nanoparticles that were used for the antibacterial tests. The samples maintained the same surface morphology following the antibacterial tests (Figure S2).

The cytotoxicity of SiO_2−Ag/PRh nanoparticles was determined from ATP analysis using human SK-BR-3 breast cancer cells (10^4 cells/mL). The production of ATP from the nanoparticle-treated cells decreased as the concentration of nanoparticles increased. As shown in Figure S3, the viability of the cells was over 76% at a concentration of 10 μg/mL and was approximately 62% at a concentration of 15 μg/mL following incubation in the SiO_2−Ag/PRh nanoparticles for 24 h. Palomäki et al. reported that the viability of macrophages treated with TiO_2 nanoparticles (30−40 nm in diameter) was in the range of 55−70% at 30 μg/mL after 24 h.[38] On the basis of these data, the cytotoxicity of the SiO_2−Ag/PRh nanoparticles was not greater than that of the TiO_2 nanoparticles.

The antibacterial activity of the SiO_2−Ag/PRh nanoparticles is attributed to silver ions and the contact-active polyrhodanine. These two distinct bactericidal mechanisms may provide an opportunity to overcome some of the disadvantages associated with each individual mechanism. For instance, the effects of the silver compound are time-limited because the silver destroys bacteria via the release of Ag^+ ions. We expect that the nanocomposites can maintain antibacterial activity after depletion of the silver component because of the existence of the polyrhodanine. Recently, Xiu et al. reported that the antimicrobial activity of silver nanoparticles depends not only on silver nanoparticles but also on the Ag(I) ions.[14] When silver is exposed to oxygen, the surfaces is oxidized, and in aqueous solution the silver oxides are dissolved and silver ions are released.[39] The released silver ions may interact with negatively charged bacterial surfaces and induce cell death.

To create a silver-depleted sample, we used a silver-ion scavenger (i.e., a neutralizer solution) in the antibacterial tests to remove the silver ions and to inhibit the bactericidal effect of the silver nanoparticles. The aim of this experiment was to indirectly observe the antibacterial properties of the polyrhodanine. Three different experimental conditions were investigated: $AgNO_3$ in solution, SiO_2−Ag/PRh nanoparticles dispersed in a solvent, and Ag nanoparticles embedded in the SiO_2 (SiO_2−Ag nanoparticles) (i.e., with no polyrhodanine) dispersed in the same solvent. (The synthetic route for the SiO_2−Ag nanoparticles is described in the Supporting Information.) The silver-ion-scavenger solution was added to the sample solution at various concentrations, and each solution was inoculated with bacteria and incubated at 37 °C for 1 h with shaking. Equal-volume aliquots were then taken from each sample and cultured on LB agar plates at 37 °C for

Table 1. Bacterial Survival Percentage of Various Silver Compounds[a] (Silver Nitrate, SiO_2−Ag, and SiO_2−Ag/PRh) and Blank Solution against *E. coli* and *S. aureus* Depending on the Amount of Neutralizer Solution (Ag Ion Scavenger)

		bacterial survival percentage (%)[c]			
bacteria	amount of neutralizer solution (μL)[b]	distilled water	$AgNO_3$	SiO_2−Ag nanoparticles	SiO_2−Ag/PRh nanoparticles
E. coli	10	98.9	1.5	0.5	2.8
	50	99.5	38.6	52	10.4
	100	96	85.8	75.8	19.7
	200	65.4	68.2	65.7	12.5
S. aureus	10	99.5	4.8	4.1	4.5
	50	98.9	60.2	45.2	27
	100	97.1	95.3	93.3	36.8
	200	72.1	75.5	78	25.2

[a]The concentration of Ag in the silver compounds was adjusted to ca. 70 μg/mL using an ICP-atomic emission spectrometer. [b]The neutralizer solution was prepared by dissolving silver-ion-scavenger molecules in distilled water (14.6 wt % sodium thiosulfate and 10 wt % sodium thioglycolate). [c]Bacterial survival percentage was calculated as $(B/A)100$ (where A is the number of bacteria colonies in the control and B is that in the sample). The standard deviation was less than 10%

24 h. Distilled water was tested under the same conditions to provide a control for the toxicity of the scavenger solution to the bacterial cells. As shown in Table 1, the bacterial survival was not influenced until the volume of the neutralizer solution increased to 100 μL. Thus, we may consider the toxicity of the silver-ion scavenger to be negligible if there was less than 100 μL. When the amount of Ag-ion scavenger increased to 100 μL, the antibacterial activity of the $AgNO_3$ and the SiO_2−Ag nanoparticles toward both *E. coli* and *S. aureus* was markedly reduced. However, the antibacterial activity of the SiO_2−Ag/PRh nanoparticles was much greater than that of the $AgNO_3$ and SiO_2−Ag nanoparticles with the silver-ion scavenger.

To confirm that it was the polyrhodanine that gave rise to the antibacterial properties, we performed antibacterial tests with pristine silica nanoparticles and silica nanoparticles that were treated with thiol-terminated silane under the same experimental conditions. As shown in Figure 4, both the pristine silica and the thiol-SiO_2 nanoparticles did not show antimicrobial properties against either bacteria regardless of the existence of the silver-ion scavenger. Therefore, we concluded that the polyrhodanine gave rise to the antibacterial activity of the SiO_2−Ag/PRh nanoparticles and that 81% of the antibacterial action toward *E. coli* and 63% toward *S. aureus* remained when the silver-ion scavenger was present.

These data demonstrate that the SiO_2−Ag/PRh nanoparticles have antibacterial action because of both the release of silver ions and the contact between the polyrhodanine and bacterial cells. Compared with the silica nanoparticles solely decorated with Ag nanoparticles, the SiO_2−Ag/PRh nanoparticles retained antimicrobial activity in the presence of a silver-ion scavenger because of the polyrhodanine.

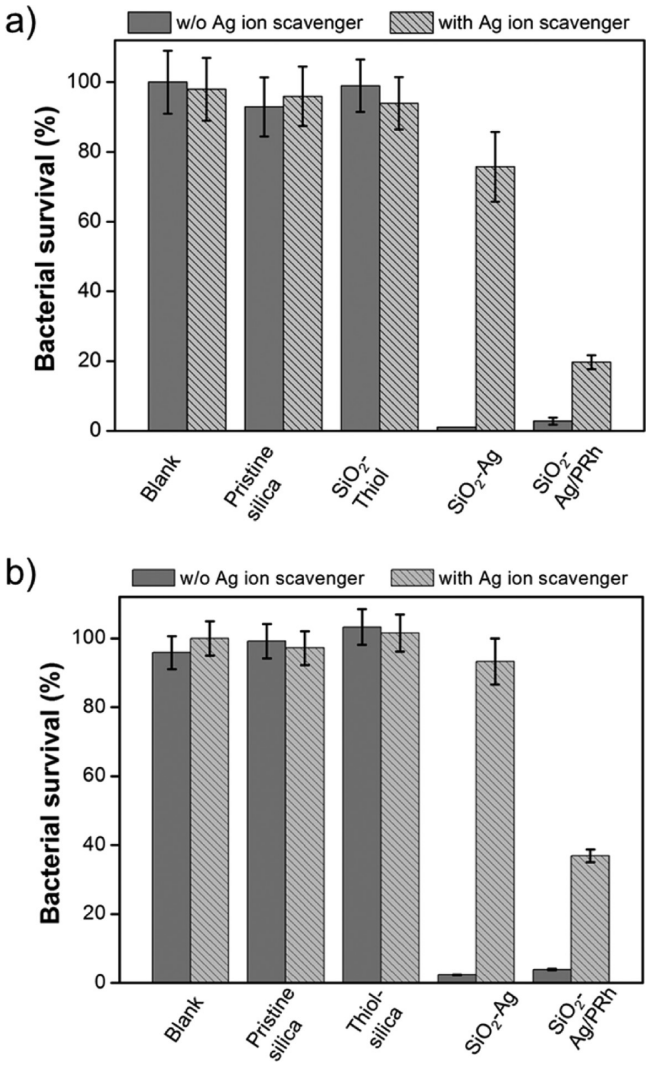

Figure 4. Antibacterial assessment of four different particles (pristine silica, thiol-silane-treated silica, SiO_2−Ag, and SiO_2−Ag/PRh) dispersed in solution and blank water toward (a) *E. coli* and (b) *S. aureus* with or without silver-ion scavenger (100 μL of neutralizer solution) at pH ca. 7.4.

CONCLUSIONS

Silver/polyrhodanine-nanocomposite-decorated silica nanoparticles were fabricated by chemical oxidation polymerization. Because the Ag^+ ion acts as an initiator, the polymerization of rhodanine occurred preferentially on the surface of the Ag^+-ion-embedded SiO_2 nanoparticles. During polymerization, the Ag^+ ions were reduced to metallic Ag nanoparticles; consequently, silver-polyrhodanine nanocomposites were formed on the silica surface.

A systematic evaluation of the antibacterial activity of the composite nanoparticles was carried out and showed excellent bactericidal properties against both gram-negative and gram-positive bacteria. Importantly, the SiO_2−Ag/PRh nanoparticles retained their antimicrobial activity even when the silver ions were depleted because of the contact-active antimicrobial activity of the polyrhodanine. These results suggest that the

SiO_2−Ag/PRh nanoparticles may be useful as a long-term antimicrobial agent.

■ ASSOCIATED CONTENT

Supporting Information

TEM image of the silver nanoparticles-decorated silica nanoparticles, TEM image of the SiO_2−Ag/PRh nanoparticles after antibacterial test, and ATP content of the synthesized nanoparticles. This material is available free of charge via the Internet at http://pubs.acs.org.

■ AUTHOR INFORMATION

Corresponding Author

*E-mail: jsjang@plaza.snu.ac.kr. Tel.: (+82) 2-880-7069. Fax: (+82) 2-888-1604.

Notes

The authors declare no competing financial interest.

■ ACKNOWLEDGMENTS

This research was supported by the WCU (World Class University) program through the National Research Foundation of Korea funded by the Ministry of Education, Science and Technology (R31-10013).

■ REFERENCES

(1) Song, J.; Kong, H.; Jang, J. *Chem. Commun.* **2009**, 5418−5420.
(2) Siedenbiedel, F.; Tiller, J. C. *Polymers* **2012**, *4*, 46−71.
(3) Timofeeva, L.; Kleshcheva, N. *Appl. Microbiol. Biotechnol.* **2011**, *89*, 475−492.
(4) Kong, H.; Song, J.; Jang, J. *Environ. Sci. Technol.* **2010**, *44*, 5672−5676.
(5) Dallas, P.; Sharma, V. K.; Zboril, R. *Adv. Colloid Interface Sci.* **2011**, *166*, 119−135.
(6) Kumar, A.; Vemula, P. K.; Ajayan, P. M.; John, G. *Nat. Mater.* **2008**, *7*, 236−241.
(7) Knetsch, M. L. M.; Koole, L. H. *Polymers* **2011**, *3*, 340−366.
(8) Park, M. V. D. Z.; Neigh, A. M.; Vermeulen, J. P.; De la Fonteyne, L. J. J.; Verharen, H. W.; Briedé, J. J.; Van Loveren, H.; De Jong, W. H. *Biomaterials* **2011**, *32*, 9810−9817.
(9) Carlson, C.; Hussain, S. M.; Schrand, A. M.; Braydich-Stolle, L. K.; Hess, K. L.; Jones, R. L.; Schlarger, J. J. *J. Phys. Chem. B.* **2008**, *112*, 13608−13619.
(10) AshaRani, P. V.; Mun, G. L. K.; Hande, M. P.; Valiyaveettil, S. *ACS Nano* **2009**, *3*, 279−290.
(11) Hackenberg, S.; Scherzed, A.; Kessler, M.; Hummel, S.; Technau, A.; Froelich, K.; Ginzkey, C.; Koehler, C.; Hagen, R.; Kleinsasser, N. *Toxicol. Lett.* **2011**, *201*, 27−33.
(12) Kawata, K.; Osawa, M.; Okabe, S. *Environ. Sci. Technol.* **2009**, *43*, 6046−6051.
(13) Hamouda, T.; Baker, J. R. *J. Appl. Microbiol.* **2000**, *89*, 397−403.
(14) Xiu, Z.; Zhang, Q.; Puppala, H. L.; Covin, V. L.; Alvarez, P. J. J. *Nano Lett.* **2012**, *12*, 4271−4275.
(15) Lv, M.; Su, S.; He, Y.; Huang, Q.; Hu, W.; Li, D.; Fan, C.; Lee, S.-T. *Adv. Mater.* **2010**, *22*, 5463−5467.
(16) Li, Z.; Lee, D.; Sheng, X.; Cohen, R. E.; Rubner, M. F. *Langmuir* **2006**, *22*, 9820−9823.
(17) Lin, J.-J.; Lin, W.-C.; Li, S.-D.; Lin, C.-Y.; Hsu, S.-H. *ACS Appl. Mater. Interfaces* **2013**, *5*, 433−443.
(18) Tang, J.; Chen, Q.; Xu, L.; Zhang, S.; Feng, L.; Cheng, L.; Xu, H.; Liu, Z.; Peng, R. *ACS Appl. Mater. Interfaces* **2013**, *5*, 3867−3874.
(19) Xu, W.-P.; Zhang, L.-C.; Li, J.-P.; Lu, Y.; Li, H.-H.; Ma, Y.-N.; Wang, W.-D.; Yu, S.-H. *J. Mater. Chem.* **2011**, *21*, 4593−4597.
(20) Yuan, W.; Jiang, G.; Che, J.; Qi, X.; Xu, R.; Chang, M. W.; Chen, Y.; Lim, S. Y.; Dai, J.; Chan-Park, M. B. *J. Phys. Chem. C* **2008**, *112*, 18754−18759.
(21) Niu, A.; Han, Y.; Wu, J.; Yu, N.; Xu, Q. *J. Phys. Chem. C* **2010**, *114*, 12728−12735.
(22) Kong, H.; Jang, J. *Langmuir* **2008**, *24*, 2051−2056.
(23) Kong, H.; Jang, J. *Biomacromolecules* **2008**, *9*, 2677−2681.
(24) Song, J.; Kang, H.; Lee, C.; Hwang, S. H.; Jang, J. *ACS Appl. Mater. Interfaces* **2012**, *4*, 460−465.
(25) Agarwal, A.; Weis, T. L.; Schurr, M. J.; Faith, N. G.; Czuprynski, C. J.; McAnulty, J. F.; Murphy, C. J.; Abbott, N. L. *Biomaterials* **2010**, *31*, 680−690.
(26) Liong, M.; France, B.; Bradley, K. A.; Zink, J. I. *Adv. Mater.* **2009**, *21*, 1684−1689.
(27) Kim, Y. H.; Lee, D. K.; Cha, H. G.; Kim, C. W.; Kang, Y. S. *J. Phys. Chem. C* **2007**, *111*, 3629−3635.
(28) Song, J.; Song, H.; Kong, H.; Hong, J.-Y.; Jang, J. *J. Mater. Chem.* **2011**, *21*, 19317−19323.
(29) Dallas, P.; Niarchos, D.; Vrbanic, D.; Boukos, N.; Pejovnik, S.; Petridis, D. *Polymer* **2007**, *48*, 2007−2013.
(30) Bober, P.; Stejskal, J.; Trchová, M.; Prokeš, J.; Sapurina, I. *Macromolecules* **2010**, *43*, 10406−10413.
(31) Kong, H.; Song, J.; Jang, J. *Macromol. Rapid Commun.* **2009**, *30*, 1350−1355.
(32) Landeen, L. K.; Yahya, M. T.; Gerba, C. P. *Appl. Environ. Microbiol.* **1989**, *55*, 3045−3050.
(33) Pearson, R. G. *J. Am. Chem. Soc.* **1963**, *85*, 3533−3539.
(34) Pandey, S.; Goswami, G. K.; Nanda, K. K. *Int. J. Biol. Macromol.* **2012**, *51*, 583−589.
(35) Sun, X.; Dong, S.; Wang, E. *Macromolecules* **2004**, *37*, 7105−7108.
(36) Wang, X.; Yu, J. C.; Ho, C.; Mak, A. C. *Chem. Commun.* **2005**, 2262−2264.
(37) Kardaş, G.; Solmaz, R. *Appl. Surf. Sci.* **2007**, *253*, 3402−3407.
(38) Palomäki, J.; Karisola, P.; Pylkkänen, L.; Savolainen, K.; Alenius, H. *Toxicology* **2010**, *267*, 125−131.
(39) Sotiriou, G. A.; Meyer, A.; Knijnenburg, J. T. N.; Panke, S.; Pratsinis, S. E. *Langmuir* **2012**, *28*, 15929−15936.